Supplementary Information for *"Surface rupture during the 2010 Mw 7.1 Darfield (Canterbury) earthquake: implications for fault rupture dynamics and seismic-hazard analysis"* by M. Quigley et al.

Derivation of Surface Rupture Length, Displacement, Magnitude, and Stress Drop for the Greendale Fault Rupture

METHODOLOGY AND DATASETS USED TO DERIVE *SRL* and *D* MEASURMENTS

We used RTK GPS and Differential (D)GPS surveying, tape measurements, and terrestrial and airborne LiDAR data (Fig. 1D in Quigley et al. 2011 and Fig. DR1-DR2 below) to map fault features and measure more than 100 horizontal (HD), vertical (VD), and net displacements (D) of formerly linear features, including roads, fences, hedge-rows, crop and tree lines, irrigation channels, tire tracks, and power lines. RTK mapping and surveying was conducted using a Leica SR 530 with horizontal and vertical accuracy of ~1-2 and 2-3 cm, respectively. Profiles were obtained by marking points at ~1 m intervals along formerly linear features such as road edges and lines of fence posts oriented at high angles to the fault trace. DGPS mapping using a Trimble GeoXH and external Zephyr antenna, with horizontal and vertical accuracies of .1-1 m and .2-2m respectively, was used to track ground ruptures in detail and ground-truth other datasets. Tape measures and compass were used to measure displacement vectors where distinct offsets were visible. An airborne LiDAR survey was conducted on September 10th by NZ Aerial Mapping using an Optech ALTM3100EA instrument at an elevation of 600m above the ground surface with a field of view of 38^{o}. Vertical accuracy of ground returns was improved from +/- 0.03 m to 0.00 m using check sites. LiDAR pixel dimensions were 0.5m. LiDAR was used to map main features, cross-check the horizontal and vertical displacements measured in the field, and produce additional vertical displacement data along the fault at numerous locations.

Displacements were measured in ArcGIS using the best available data at over 100 sites. For HD, straight lines were projected through the surveyed feature away from the fault, copied onto the corresponding feature on the other side of the fault, and their separation measured along a generalised fault line. Uncertainties were inferred to take into account the measurement uncertainties (above), as well as the data fit and data type. Horizontal RTK GPS field measurements have a lower uncertainty than those obtained from LiDAR data and thus most of the HD values are from field data. VD were generally measured from profiles

extracted from the LiDAR (cross-checked against the typically shorter RTK GPS profiles), and were undertaken using the same methodology as the HD. VD uncertainties are generally higher than HD because of the channelized topography of the alluvial plain surface and the inherent lesser accuracy of the LiDAR compared to field data.

Average displacements (D_{avg}) were calculated using the area beneath a suite of curves that fit all displacement data. The average surface displacement along the fault is estimated to be 2.5 +/- 0.1m (2 sigma limits). This estimate was obtained from the mean and standard deviation of 1000 simulations of the average surface displacement. In each simulation, a sample was drawn from the uncertainty distribution of each observed displacement and that of the two end-points, and linear changes in displacement were assumed along the fault between the observed values. Some other surface rupture investigations have often tended to weigh the higher values more than adjacent lower values. In such investigations, the rationale typically offered is that the lower values are underestimates because some distributed deformation was not captured by the displacement marker at that site, whereas, the higher values are more likely to be the ones recording a true estimate of the full displacement at that site. This may not be as relevant in our case, as the abundant linear markers provided a remarkable framework to document displacements even over large (>100m) deformation zone widths. In order to gain an indication of what the variability of our D_{avg} value might be, we also tried a more extreme curve that basically is a straight line fit through the high values. This more extreme curve satisfies (again within uncertainty) all our high values, but misses out a few more of the low values. The D_{avg} resulting from this scenario is 2.8 m. This value of 2.8 m is likely to represent a robust estimate of a maximum bound for D_{avg}. To gain an indication of what the minimum bound of D_{avg} is, we considered the scenario that perhaps surface rupture was 1 km longer (30.5 km compared to 29.5 km) and that this extra km of rupture had negligible (zero) displacement. We used the displacement curve that we use to derive our D_{avg} value of 2.5 m, and added an extra km to that with zero displacement. The resulting D_{avg} is 2.4 m. If 2 km of rupture with zero displacement is added then the resulting D_{avg} is 2.3 m. Adding 1 km to rupture length is possibly supported by our statements/observations of uncertainty about rupture length, but adding 2 km is overly extreme, and not supported by our data and observations. In conclusion, estimates of D_{avg} for the Greendale Fault range between 2.4 m to 2.8 m (at ~ 95% conference), however the average surface displacement along the fault is estimated to be 2.5 +/- 0.1m (2 sigma limits) using 1000 simulations. We report the D_{avg} as 2.5 +/- 0.1 m in Quigley et al. (2011).

JUSTIFICATION FOR LOCATION OF FAULT RUPTURE TIPS AND UNCERTAINTY IN MAPPED SRL

The abundance of formerly linear features, including roads, fences, hedge-rows, crop and tree lines, irrigation channels, tire tracks, and power lines in the study area allowed the rupture tips of the Greendale Fault to be identified with high precision. Maps used to define the eastern extent of rupture show Hoskyns Road (43.573°S, 172.375°E) and fences to the east appear to be un-deformed, whereas fences to west are. Based on these, the uncertainty of the location of eastern end of surface rupture is +/- 100 metres. At the western end, using the same methodology, we estimate that the uncertainty on the location of the western rupture tip is +/- 450 metres. The trace could not be 1 km longer at western end; at a distance 1 km NW from the mapped end point there are lots of long straight fences that were not deformed. We thus report a *SRL* of 29.5 ±0.5 km in Quigley et al. (2011).

DERIVATION OF M_w^G AND $\Delta\sigma^G$ USING GEOLOGIC DATA

To investigate whether we would have accurately estimated the M_w potential of the GF from surface rupture characteristics alone, as would be employed in paleoseismic analysis, we used the *SRL*, D_{max}, and D_{avg} versus M_w regressions from global strike-slip earthquakes to derive 'geologic' estimates of moment magnitude (M_w^G);

$M_w^G = 5.16\ (\pm 0.13) + 1.12\ (\pm 0.08) * \mathrm{Log}\ (SRL)$ (1) (Wells and Coppersmith, 1994)

$M_w^G = 6.81\ (\pm 0.05) + 0.78\ (\pm 0.06) * \mathrm{Log}\ (D_{max})$ (2) (Wells and Coppersmith, 1994)

$M_w^G = 7.04\ (\pm 0.05) + 0.89\ (\pm 0.09) * \mathrm{Log}\ (D_{avg})$ (3) (Wells and Coppersmith, 1994)

$M_w^G = 5.56 + 0.87 * \mathrm{Log}\ (SRL)$ (4) (Wesnousky, 2008)

Using (1), we find $M_w^G = 6.8 \pm 0.2$ for *SRL* and $M_w^G = 6.6 \pm 0.2$ for SRL_{min}. Using (2) we find $M_w^G = 7.4 \pm 0.1$. Using (3) we find $M_w^G = 7.4 \pm 0.1$. Using (4) we find $M_w^G = 6.8$ for *SRL* and $M_w^G = 6.7$ for SRL_{min}. M_w^G was also determined using:

$M_w^G = (\mathrm{Log}\ (\mu LWD_{avg}) - 16.05)/1.5$ (5) (Hanks and Kanamori, 1979)

where the crustal rigidity (μ) = 3×10^{11} dyne/cm^2, rupture width (W), as derived from aftershock maximum depth distributions (Gledhill et al., 2011) = 12 ± 2 km, subsurface fault length (L) = 4/3*SRL* = 39.3km (consistent with geodetically derived estimates of 40 km for

Greendale *L*; Beavan et al., 2010), and D_{avg} = 250cm, giving M_w = 7.0 ± 0.1 for *SRL* and 6.9 ± 0.05 for SRL_{min}. Finally, we used the regression equation used in the New Zealand seismic hazard model (Stirling et al., 2008):

$M_w^G = 4.18 + 2/3\text{Log}W + 4/3\log L$ (6) (Berryman et al., 2002)

and find M_w^G = 7.0 ± 0.1 for $L = 4/3SRL$ and 6.9 ± 0.1 for $L = 4/3SRL_{min}$.

Uncertainties in the conversion of *SRL* to *L* broaden the error range in M_w estimates using (5) and (6).

Beavan et al. (2010) calculated the GF-only M_w = 7.0 using a GPS and InSAR-derived fault source model. *SRL*-based regressions (1,4) thus underestimate the Darfield earthquake M_w and are at the low end, albeit within error, of the GF-only M_w (4). SRL_{min} regressions (1,4) significantly underestimate M_w. D_{max} and D_{avg} regressions (2,3) significantly overestimate M_w. Equations using *W, L* (5,6) and D_{avg} (5) provide *SRL*-based estimates within error of M_w and SRL_{min} -based estimates below M_w and within error of the GF-only M_w.

We also used surface rupture data to calculate a 'geologic' estimate of co-seismic static stress drop on the GF rupture ($\Delta\sigma^G$):

$\Delta\sigma^G = (\mu/C) \times (D_{avg}/W)$ (7) (Madariaga, 1977)

where *C* is a function of the aspect ratio of a longitudinal elliptical fault geometry, derived using first kind *E(k)* and second kind *K(k)* complete elliptical integrals and $k = \sqrt{1 - W^2/L^2}$:

$C = 4[3E(k) + ((K(k) - W^2/L^2E(k))/k^2]^{-1}$ (8) (Madariaga, 1977)

We derive $\Delta\sigma^G$ = 13.9 ± 3.7 MPa using this method.

FOOTNOTE

A destructive aftershock of local magnitude (M_L) 6.3 and shallow depth struck approximately 10 km southeast of the Christchurch CBD at 12:51 on Tuesday 22 February 2011 local daylight time (23:51 on 21 February UT), causing extensive damage and 182 fatalities (Gledhill et al., 2011). Another large aftershock (M_L 6.0) struck on June 13th. These events are a poignant reminder of the challenges of earthquake analysis in relatively low

strain rate regions; no surface rupture has been found to date for either rupture and there was no prior evidence for large paleo-earthquakes on these faults. These earthquakes occurred in a region of low to moderate seismicity that has a strong earthquake preparedness culture (in terms of monitoring and compliance of seismic design codes), given its reasonable proximity to a fast slipping plate boundary. However, other areas worldwide with similar levels of seismicity that are either far away from a plate boundary, or within a slow slipping plate boundary, may not be ready for similar moderate magnitude earthquakes capable of extreme destruction.

LiDAR PLATES

Figure Captions

Fig. DR1. Mapped surface trace of the Greendale fault from Quigley et al. (2010[b]) and Van Dissen et al. (2011). Red arrows indicate relative sense of lateral displacement, while vertical displacement is denoted by red U = up and D = down. Locations of Figures DR2A-E shown as boxes and Darfield earthquake epicentre as red star (Gledhill et al. 2011).

Fig. DR2. LiDAR hillshade DEMs (illuminated from the NW) of three ~1.8 km long (A, C, E) and two ~1.5 km long (B, D) sections of the Greendale Fault. Images show characteristic left-stepping en echelon rupture pattern and dextral offset of roads, fences, irrigation channels, hedges and crop rows. Examples of fault step-overs and push-up "bulges" described in Quigley et al. (2011) are clearly visible. The general amount of net surface rupture displacement in A, B-D, and E is, respectively, 1.5 to 2.5 m (horizontal to vertical ratio ~3:1, south side up), 4 to 5 m (predominantly dextral), and 4 to 2.5 m (predominantly dextral). LiDAR from NZ Aerial Mapping Limited. Images A, C, and E from Van Dissen et al. (2010), B from Quigley et al. (2010[a], 2010[b]), and D from Quigley et al. (2010[b]). Numerous field photographs of the surface rupture are available in Barrell et al. (2011).

Figures

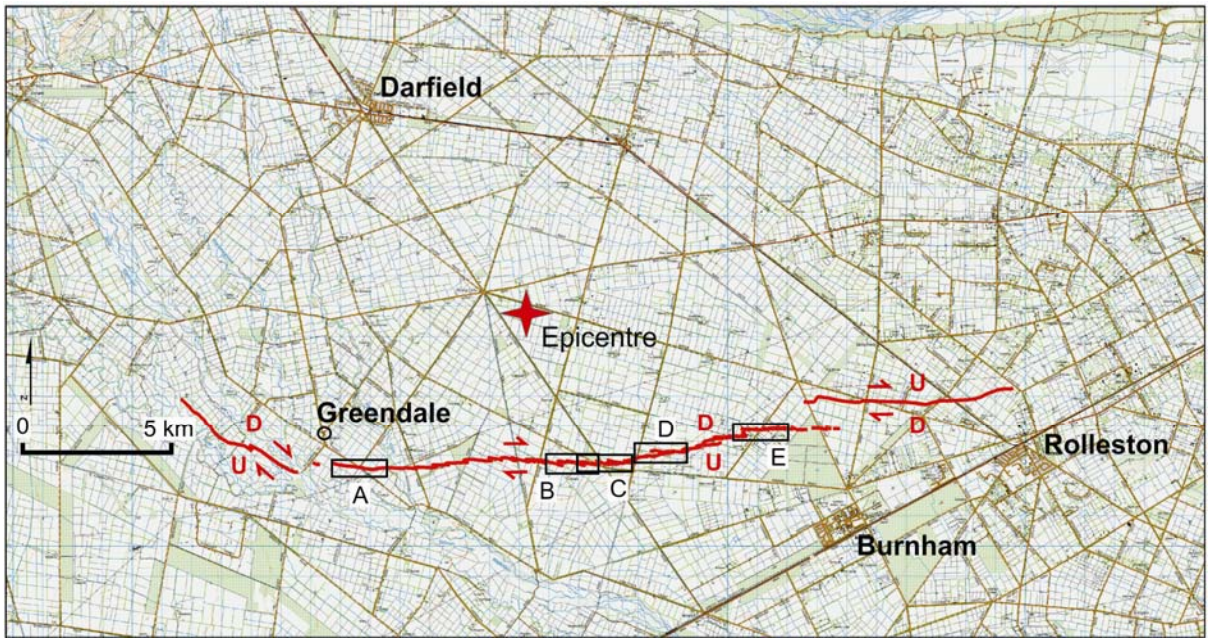

Fig. DR1. Mapped surface trace of the Greendale fault

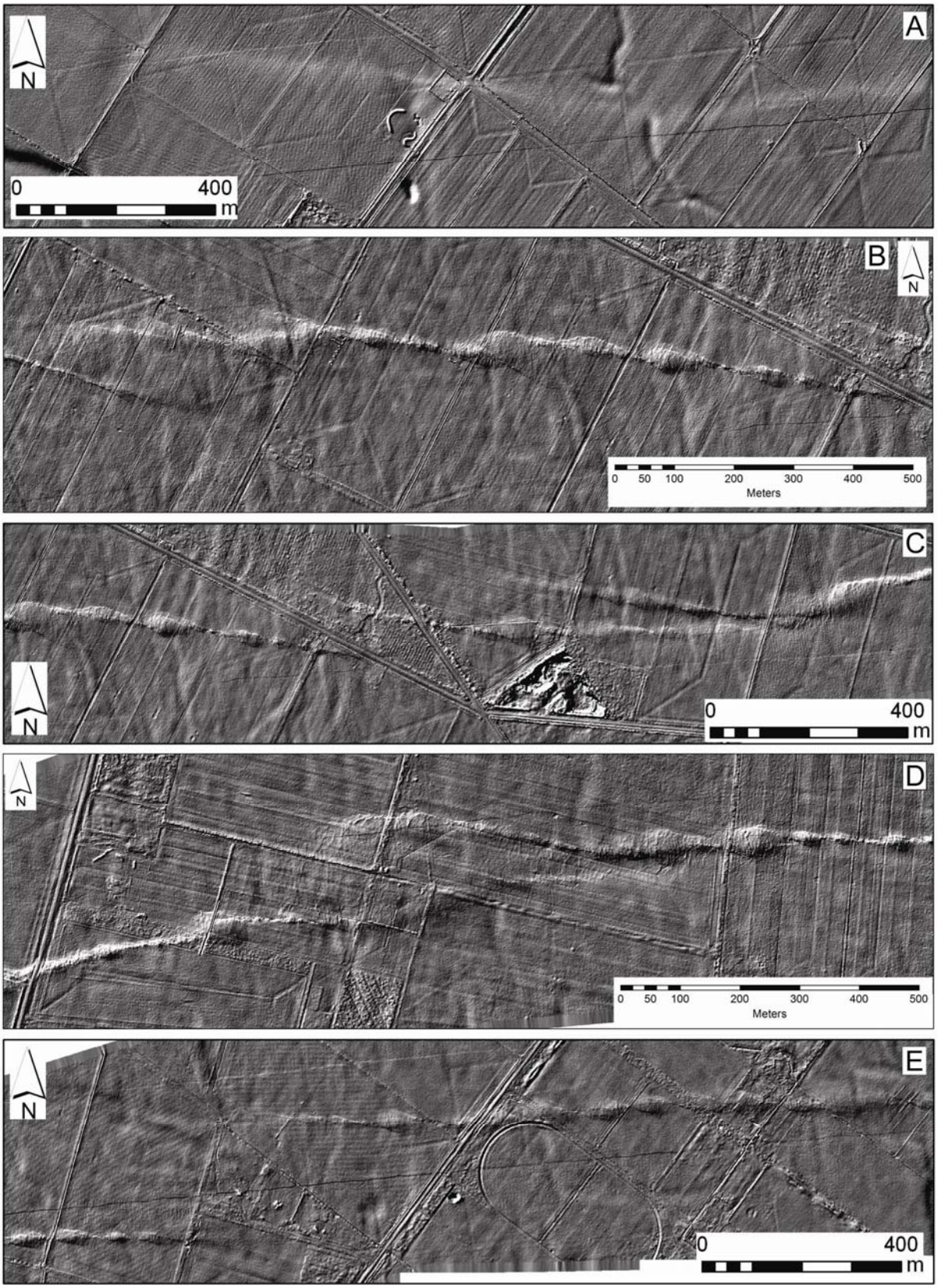

Fig. DR2. LiDAR hillshade DEMs of Greendale Fault surface rupture

REFERENCES

Beavan, J., Samsonov, S., Motagh, M., Wallace, L., Ellis, S., and Palmer, N., 2010, The Mw 7.1 Darfield (Canterbury) earthquake: Geodetic observations and preliminary source model: Bulletin of the New Zealand Society for Earthquake Engineering, v. 43, p. 228–235.

Berryman, K., Webb, T., Hill, N., Stirling, M., Rhoades, D., Beavan, J., and Darby, D., 2002, Seismic loads on dams, Waitaki system, Earthquake Source Characterisation: GNS client report 2011/129, 80 p.

Barrell, D., Litchfield, N.J., Townsend, D.B., Quigley, M., Van Dissen, R.J., Cosgrove, R., Cox, S.C., Furlong, K., Villamor, P., Begg, J.G., Hemmings-Sykes, S., Jongens, R., Mackenzie, H., Noble, D., Stahl, T., Bilderback, E., Duffy, B., Henham, H., Klahn, A., Lang, E.M.W., Moody, L., Nicol, R., Pedley, K., Smith, A., 2011, Strike-slip ground-surface rupture (Greendale Fault) associated with the 4th September 2010 Darfield Earthquake, Canterbury, New Zealand: Quarterly Journal of Engineering Geology and Hydrogeology, v. 44; p. 283-291.

Gledhill, K., Ristau, J., Reyners, M., Fry, B., and Holden, C., 2011, The Darfield (Canterbury, New Zealand) Mw 7.1 earthquake of September 2010: A preliminary seismological report: Seismological Research Letters, v. 82, p. 378–386.

Hanks, T.C., and Kanamori, H., 1979, A moment magnitude scale: Journal of Geophysical Research, v. 84, p. 2348–2350, doi:10.1029/JB084iB05p02348.

Madariaga, R., 1977, Implications of stress-drop models of earthquakes for the inversion of stress drop from seismic observations: Pure and Applied Geophysics, v. 115, p. 301–316, doi:10.1007/BF01637111.

Quigley, M., Van Dissen, R., Litchfield, N., Villamor, P., Duffy, B., Barrell, D., Furlong, K., Stahl, T., Bilderback, E., Noble, D., 2011, Surface rupture during the 2010 Mw 7.1 Darfield (Canterbury, New Zealand) earthquake: implications for fault rupture dynamics and seismic-hazard analysis: Geology, 4 p.

Quigley, M., Villamor, P., Furlong, K., Beavan, J., Van Dissen, R., Litchfield, N., Stahl, T., Duffy, B., Bilderback, E., Noble, D., Barrell, D., Jongens, R., Cox, S., 2010[a], Previously Unknown Fault Shakes New Zealand's South Island, Eos, Transactions, American Geophysical Union, Vol. 91, No. 49, p.469-471

Quigley, M., Van Dissen, R., Villamor, P., Litchfield, N., Barrell, D., Furlong, K., Stahl, T., Duffy, B., Bilderback, E., Noble, D., Townsend, D., Begg, J., Jongens, R., Ries, W., Claridge, J., Klahn, A., Mackenzie, H., Smith, A., Hornblow, S., Nicol, R., Cox, S., Langridge, R., Pedley, K., 2010[b], Surface rupture of the Greendale Fault during the Mw 7.1 Darfield (Canterbury) Earthquake, New Zealand: initial findings: Bulletin of the New Zealand Society for Earthquake Engineering, v 43(4), p. 236-242.

Stirling, M., Gerstenberger, M., Litchfield, N., McVerry, G., Smith, W., Pettinga, J., and Barnes, P., 2008, Seismic hazard of the Canterbury region, New Zealand: New earthquake source model and methodology: Bulletin of the New Zealand Society for Earthquake Engineering, v. 41, p. 51–65.

Van Dissen, R., Barrell, D., Litchfield, N., Villamor, P., Quigley, M., King, A., Furlong, K., Begg, J., Townsend, D., Mackenzie, H., Stahl, T., Noble, D., Duffy, B., Bilderback, E., Claridge, J., Klahn, A., Jongens, R., Cox, S., Langridge, R., Ries, W., Dhakal, R., Smith, A., Hornblow, S., Nicol, R., Pedley, K., Henham, H., Hunter, R., Zajac, A., Mote, T., 2011, Surface rupture displacement on the Greendale Fault during the Mw 7.1 Darfield (Canterbury) earthquake, New Zealand, and its impact on man-made structures:.*In* Proceedings of the 9th Pacific Conference on Earthquake Engineering, Auckland, New Zealand, 14-16 April, 2011: Paper 186, 8 p.